PROCEEDINGS, 50th Workshop on Geothermal Reservoir Engineering
Stanford University, Stanford, California, February 10-12, 2025
SGP-TR-229

Flow Measurements and Transport of Temperature-Responsive Hydrogel Microspheres for Use in Subsurface Flow Management

Bryan H. Abdulaziz[1], Aaron Baxter[1], Adam J. Hawkins[4], Danni Tang[2], Sarah Hormozi[1], Patrick Fulton[3], Ulrich B. Wiesner[2], Jefferson W. Tester[1]

Robert Frederick Smith School of Chemical & Biomolecular Engineering[1], Materials Science & Engineering[2], Earth & Atmospheric Sciences[3], College of Engineering, Cornell University, 113 Ho Plaza, Ithaca, NY 14850, USA

School of Civil and Environmental Engineering and Earth Sciences, College of Engineering, Computing and Applied Sciences, Clemson University, Clemson, SC 29625, USA[4]

bha38@cornell.edu

Keywords: premature thermal breakthrough, short circuit, microgel, hydraulic control, frictional power loss, pressure drop, temperature, volume fraction, jamming

ABSTRACT

Enhanced Geothermal Systems (EGS) offer a globally scalable option to increase the energy production from Earth's internal heat. Their growth potential, however, is limited by financial risks imposed by uncertain subsurface reservoir conditions, especially the spatial distribution of fluid flow paths in fracture-dominated reservoirs. Recent work by the co-authors suggests that flow paths can be hydraulically controlled by introducing an "active" tracer that selectively swells and jams cooled regions of the reservoir thus redirecting fluids to hot regions and increasing production well temperatures. Here, we investigate the behaviour of these novel, micron-sized hydrogel microspheres passing through channels with temperature below the volume-phase-transition temperature. Specially, we were interested in seeing if they can be used to reduce short-circuited flow paths when microgel volume fractions are below and at the conditions necessary for jamming. Flow resistance effects were observed by injecting microgels into a bench-scale microfluidic setup simulating an EGS reservoir. Measurements of the pressure drop, fluid density, and mass flow rate at specified temperatures and microgel volume fractions were performed to estimate the resulting frictional power loss after a volume of the microgel injectate had migrated into the system. The data acquisition over time allows us to see if the injection conditions yield jamming. If jamming was not observed, the estimated friction power loss can be correlated with microgel volume fraction and temperature to evaluate the effectiveness of the microgels in resisting flow.

1. INTRODUCTION

Geothermal energy is a promising alternative to achieve affordable and sustainable energy security. Its low carbon footprint compared to fossil fuels and potential use as a baseload power and heating source makes it more attractive compared to variable renewable energy sources (VREs) such as wind and solar. Advances in Enhanced Geothermal Systems (EGS), which stimulates drier and less permeable rocks than conventional geothermal systems, expands the accessibility of geothermal energy to more regions around the world without the sufficient subsurface characteristics of conventional geothermal. However, the implementation of EGS is limited by uncertainties in subsurface conditions.

As working fluid flows through fractures in the system, it absorbs heat from the rock surrounding it. Over time, low overall permeability promotes the flow in fractures with least resistance, potentially improving fracture transmissivity and hydraulic performance but cooling down the surrounding rocks and, as a consequence, reducing production well temperatures (Hawkins et al., 2023; McLean & Espinoza, 2023). This premature thermal breakthrough can significantly shorten the thermal lifetime of an EGS reservoir, as production well temperatures can drop below its design/operating specifications much earlier than expected due to these thermal "short-circuits".

Simulations of flow redistribution in a geothermal reservoir by Hawkins et al., (2024) based on a numerical simulator developed by Fox et al., (2015) showed a possibility of preventing "short-circuits" in an EGS reservoir and improving its commercial lifetime. The study demonstrated the thermal evolution of a geothermal injection-production well pair after over 30 years of operation in a reservoir based on Blue Mountain, with well separation distance of 75 m, injection temperature of 40°C, and initial temperature of 130°C. To simulate the anticipated benefits of the hydraulic control treatment, regions with temperatures below 110°C were identified and the corresponding fracture apertures were reduced by a factor of 30. This hydraulic control treatment forced the circulating fluids to flow away from the short-circuited region to hotter regions, increasing the heat transfer surface area and production well fluid temperatures. Figure 1 shows a temperature contour map in the reservoir after 30 years of operation for two cases: without the hydraulic control treatment and one with the treatment. Figure 2 displays the difference in production well temperature and illustrates the anticipated improvements to commercial lifetime.

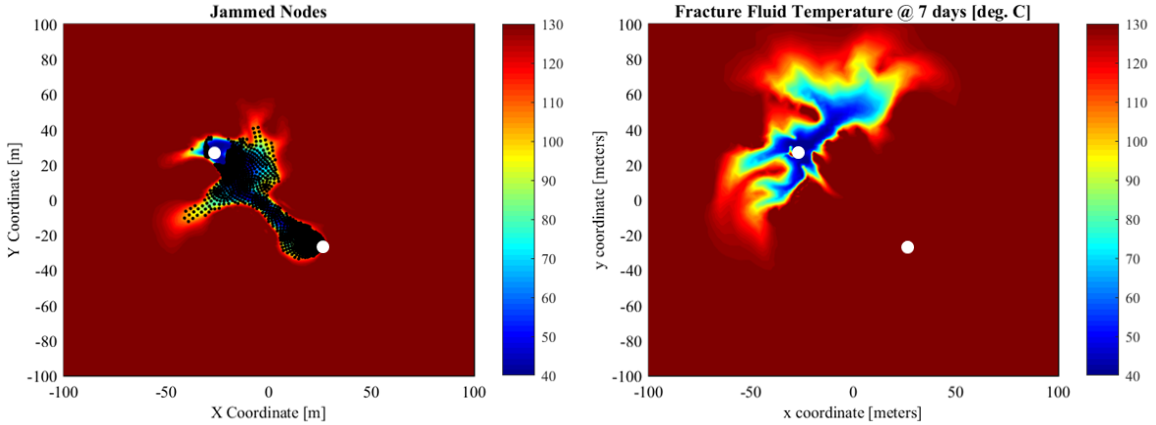

Figure 1: Simulated fracture fluid temperature distributions before the hydraulic control treatment (left) and after (right). Spatial coordinates are in meters and temperatures range from 40°C (blue) to 130°C (red). Injection and production wells are indicated by white dots in the upper left and bottom right respectively. Black dots denote "jammed nodes" with reduced apertures to redirect flow (Hawkins et al., 2024)

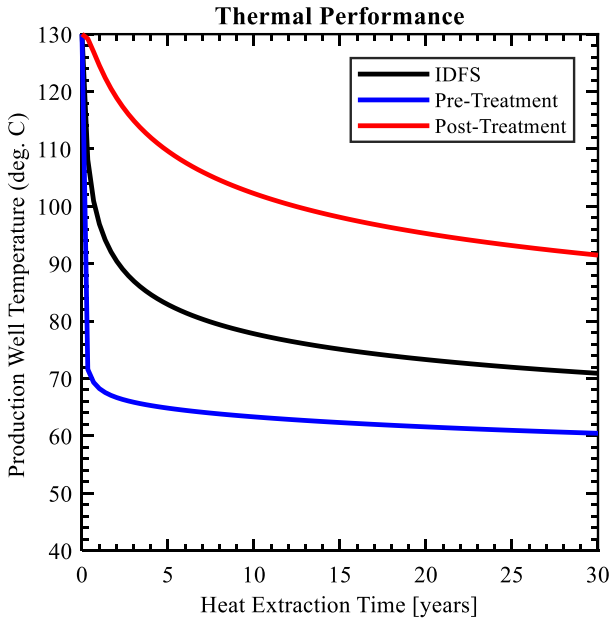

Figure 2: Simulated production well fluid temperature evolution over time of heat extraction (Hawkins et al., 2024)

The study by Hawkins et al. (2024) showed that flow redistribution is a promising solution for thermal interference and to improve EGS commercial lifetime and utilization. However, no established material and well-studied approach to apply this method has been developed yet. A key mechanism in flow redistribution is reducing apertures in a fracture that has a temperature below a certain threshold. Hawkins et al. (2024) proposed the use of "smart" polymer microgels that would swell and shrink at a certain temperature to induce this mechanism by reducing apertures and block cooled fractures, redirecting fluid flow to hotter regions in the process. Baxter et al., (2023) expanded on this study, characterizing the rheological properties of these microgels and demonstrating their capability to form yield-stress fluid that would effectively block cooled fractures.

The temperature-responsive material employed in this active tracer, which was pioneered by Tanaka (Tanaka, 1978; Tanaka et al., 1980; Yeghiazarian et al., 2005), is made of polymerized N-isopropylacrylamide (NIPA) in a cross-linked network. The key characteristic of this gel material is its temperature-responsive volume-phase-transition (VPT), where the gel counter-intuitively shrinks at temperatures above a lower critical solution temperature (T_{LCST}) and reversibly swells at temperatures below it. T_{LCST} and volumetric swelling ratio of the gel can be increased by adding sodium acrylate (SA), a property that is tuneable and has been explored extensively by Shibayama & Tanaka (1993). This controllable parameter is crucial in synthesizing the optimal microgels to swell and reduce short-circuited geothermal systems at the desired control temperature.

A rheological study by Baxter et al. (2023) showed that pNIPA-SA microgel suspensions are capable of forming a yield stress fluid below T_{LCST}. A yield stress fluid behaves like a solid when it experiences a shear stress below the value of its yield stress but exhibits plastic deformation and/or liquid-like flow when the applied shear stress is greater than its yield stress. This property enables the microgels to block or "jam" a short-circuited aperture, redistributing fluid flow out of the affected aperture. The VPT behavior of the microgel ensures that the yield stress fluid only forms when the microgels are swollen, thus selectively blocking cooled flow paths while allowing fluid to flow freely in sufficiently hot fractures.

2. RESEARCH HYPOTHESIS

The controllable properties of pNIPA-SA microgel, its VPT behavior, transport behavior at concentrations below the minimum jamming fraction, and ability to form a yield stress fluid makes it an ideal material to implement flow redistribution in a short-circuited EGS reservoir. Numerous rheological studies have provided adequate knowledge on the characteristics and behavior of these microgels (Baxter et al., 2023; Minami et al., 2016; Shu et al., 2013). Nonetheless, the capabilities of the microgels have not yet been tested under the influence of hydrodynamic dispersion in long, narrow flow paths, particularly when the diameters of the particles are close in size to the conduits hydraulic diameter. Thus, this study aims to investigate changes in frictional power loss and the relationships between these losses and jamming. The objectives of this study are to: 1.) quantify the relationship between frictional power loss and the injection conditions (e.g., volume fraction and temperature, $\dot{E}(\phi, T)$) and 2.) demonstrate hydraulic control by jamming a cold flow path and redirecting the suspension of shrunken-state particles through a high-temperature flow path.

From a macroscopic perspective, one can readily determine the frictional power loss of a flowing suspension based on the relationship between frictional pressure drop (ΔP), mass flow rate ($\dot{m}$), and fluid mass density (ρ_f) such that:

$$\dot{E} = \frac{\Delta P \dot{m}}{\rho_f} \tag{1}$$

The frictional power loss describes the effective resistance which a fluid must overcome in order to travel at a particular flow rate. In the context of the experiments presented here, Equation 1 enables one to quantify how various injection conditions effect the power necessary to flow for any combination of pressure drop and mass flow rate. Change in fluid density is assumed to be negligible in this study as the microgel volumes are relatively small compared to the circulation system. This power loss parameter can describe the intended effect of the hydrogel microspheres resisting fluid flow and, in high enough concentration, stop the flow and redirect it. Thus, this study hypothesizes that the introduction of microgel suspensions into a circulating system will add resistance to the resulting flow and lead to one of at least three scenarios, including: 1.) complete jamming of the local flow path such that the microgel suspension and the bulk fluid become stationary; 2.) incomplete jamming in which the microgels remain stationary but the surrounding fluids continue to travel in-between the hydrogel microspheres; or 3) an increase in the apparent viscosity of the bulk fluid where both the microgels and the surrounding fluids continue to travel through the flow paths, but increase the frictional power loss (Figure 3).

Because any of these three distinct possibilities could exist, one must consider three different microscopic models to relate Eq. 1 to a constitutive equation that appropriately represents the system. In the case where the suspension of microgels travels along with the bulk fluid, one can employ a hydrodynamic model that treats the changes in frictional power loss to changes in an "apparent" viscosity. One such model is the Hagen-Poiseuille equation for laminar fluid flow in a circular conduit. The treatment of such flows generalized for arbitrary shapes in Hawkins (2024) defines frictional power loss as:

$$\dot{E} = N_{Po} \dot{m} D_f \left(\frac{A_s \Delta x}{V_r}\right)^2 \nu_{obs} \tag{2}$$

where N_{Po} is the Poiseuille number (which is 2 for a circular pipe), D_f is the apparent kinematic viscosity (or momentum diffusivity) of the bulk fluid $\left[\frac{\mathrm{m}^2}{\mathrm{s}}\right]$, A_s is interfacial surface area, Δx is the fluid displacement distance (i.e., pipe length), V_r is the volume of the circulating fluid, and $\nu_{obs} = \frac{\dot{x}}{\Delta x}$.

Instead of travelling in unison, the microgels may remain stationary while the surrounding water flows through the interstitial spaces. In this circumstance, the appropriate constitutive equation should describe porous media flow following Darcy's law. Darcy's law can be recovered from Eq. 2 by substituting $k = \frac{1}{N_{Po}}\left(\frac{V_r}{A_s}\right)^2$, which yields

$$\dot{V} = \frac{k A_x}{\eta} \times \frac{\Delta P}{\Delta x} \tag{3}$$

where $\dot{V}$ is volumetric flow rate [m^3/s], k is permeability [m^2], A_x is the cross-sectional area of the porous media, η is dynamic viscosity [$\mathrm{Pa.s}$], and Δx is the length of the porous media.

In the third and final possibility, both the microgels and any interstitial fluids become immobile in the cold flow paths and the channel is effectively "jammed" which forces circulating fluids to be redirected to one or more alternative flow paths, assuming alternative paths exist. Such microscopic behavior can be modelled as a non-Newtonian, yield-stress fluid (e.g., Herschel-Bulkley fluid). This behavior is known to emerge in complex fluids when a suspension's volume fraction exceeds a critical point (Baxter et al., 2023). At fractions larger than this critical "jamming" fraction (ϕ_{jam}), the microgel suspension forms a yield stress fluid, blocking flow off the targeted flow path as long as local shear stresses remain lower than the yield stress. The Herschel-Bulkley model describes non-Newtonian fluid as such:

$$\begin{aligned} \dot{\gamma} &= 0 \qquad ,if\ \tau < \tau_y \\ \tau &= \tau_y + K\dot{\gamma}^n \quad ,if\ \tau \geq \tau_y \end{aligned} \tag{4}$$

where τ is shear stress [Pa], τ_y is the yield stress, K is the consistency index in the units of [Pa.s^n], and n is the flow index.

Baxter et al. (2023) demonstrated that the novel hydrogel microspheres employed here can be modelled as a Herschel-Bulkley fluid by utilizing a rheometer while varying mass fractions and shear rates. The study qualitatively showed the transition of the suspension from a yield stress fluid to a fluid without a yield stress through dilution at 20°C, well below T_{LCST}. In the study presented here, the injection conditions of the suspension are varied and frictional power loss is monitored. The results of this study can then be used to identify which microscopic behavior exists for ranges of injection conditions.

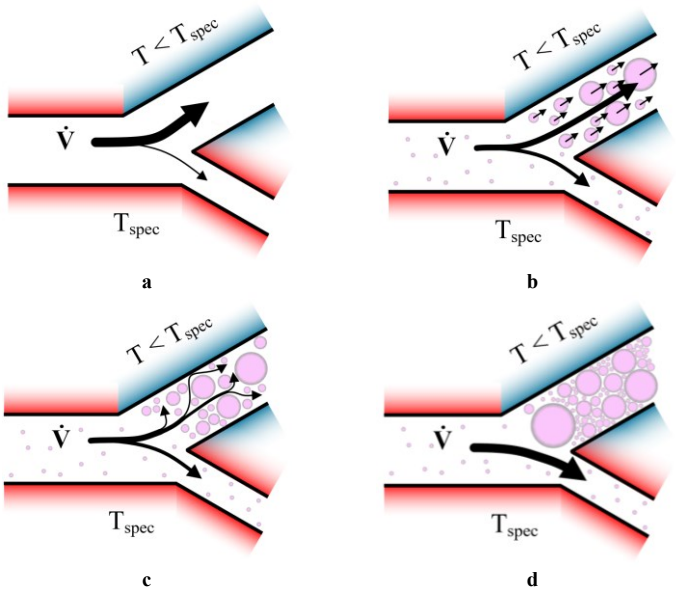

Figure 3: Schematic illustration of the untreated circumstance (a) compared to the three possible microscopic circumstances (b, c, and d). In the untreated state, fluid flow is concentrated into the larger, cold flow path. If the microscopic behavior follows the picture shown in (b), then the hydrogel microspheres swell in the cold region and increase flow through the narrower flow path, but remain in a flowing state along with the surrounding fluids. In an alternative circumstance where the microspheres are trapped in the cold flow path, fluids still travel through the interstitial spaces of the cooled path and fluid flow through the hot path is again increased (c). The third possibility is that the hydrogel suspension swells in the cooled flow path and forms a yield stress fluid that completely "jams" the cold flow path and redirects 100% of circulating fluids through the narrow, hot path.

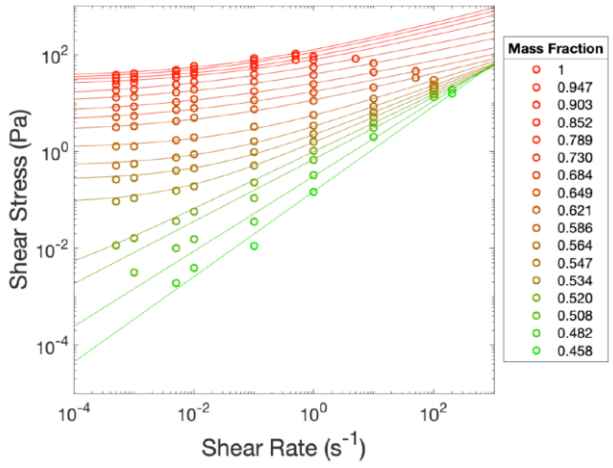

Figure 4: log-log plot of shear stress vs. shear rate of 90:10 pNIPA-SA microgel suspension without clay, and 1.29 g/L BIS with a rheometer. Mass fraction of 1 is equivalent to the maximum microgel volume fraction able to be achieved through vacuum filtration (ϕ_{max} in this study), and subsequent lower mass fractions denote dilution of this initial value by mass (Baxter et al., 2023)

3. METHODOLOGY

3.1. Injectate Preparation and Injection

A range of injection conditions was prepared to investigate viable injection strategies relevant to commercial-scale geothermal operations. All six of the experiments discussed here included an injectate consisting of pNIPA-SA microgel suspensions at a determined concentration to be injected into a simulated EGS reservoir. The hydrogel microspheres used in this study were synthesized by the project team following the procedures discussed in Baxter et al. (2023). The synthesis includes the NIPA monomer as well as sodium acrylate (NIPA:SA ratio = 98:2) and two crosslinkers (inorganic clay crosslinkers "NC" and organic crosslinkers "OR" relative abundance = $NC_{2.0}$-$OR_{0.6}$). As described in Hawkins et al. (2024), the resulting Lower Critical Solution Temperature (LCST) is 43 ℃ and the mean diameter and three-dimensional swelling ratios in a 3.5% sodium-chloride brine are 75-800 um and ~713x, respectively.

Table 1: Injectate concentrations and pre-treatment for frictional power loss experiments

Experiment Number	Volume fraction	Pre-treatment	
		Vacuum Filtration	Shrunken-State Injection
1	$0.03\phi_{max}$	No	No
2	$0.1\phi_{max}$	No	No
3	$0.3\phi_{max}$	Yes	No
4	$0.5\phi_{max}$	Yes	No
5	ϕ_{max}	Yes	No
6	ϕ_{max}	Yes	Yes – 50% bulk water volume reduced

The injectate is prepared by diluting a concentrated suspension of the "as-prepared" microgels in a synthetic brine using a pH 6 buffer solution composed of water and sodium phosphate. For the six experiments, five distinct volume fractions were prepared, including: $0.03\phi_{max}$, $0.1\phi_{max}$, $0.3\phi_{max}$, $0.5\phi_{max}$, and ϕ_{max}. ϕ_{max} represents the maximum microgel volume fraction that can be achieved in this experimental study via pretreatment. The maximum and minimum of this range were selected to investigate how dilution of the injectate affects the performance of the hydraulic control experiments.

Volume fraction is determined as a volume ratio of microgels to the total volume of the injectate. ϕ_{max} is achieved by vacuum filtrating "as-prepared" bulk material consisting of fully-swollen hydrogel microspheres and interstitial water, thereby removing excess of the latter from the former. Injectates with volume fractions above $0.1\phi_{max}$ are prepared by vacuum-filtering "as-prepared" bulk material and diluting them back to a suspension at the desired volume fraction. The injectate is then transferred into a 5.5-mL injection loop using a syringe and then introduced into the system by switching the injection valve into "injection" mode.

Experiment 6 aims to investigate the effect of injecting the particles in the shrunken state. Injecting the particles in the shrunken state is desirable, because one can introduce a highly-concentrated, shrunken-state suspension which has the capacity to swell to a volume much larger than the volume of the injection valve. When this concentrated suspension swells in a small, confined space with less "free" water volume than required to reach full swelling capacity, it reaches a "kinetically-trapped" state. The kinetically-trapped suspension consists of underswollen microgels being more tightly packed in the limited available volume, providing higher resistance to shear induced by the flow. As a result, a jam in a cooled region can occur. Therefore, this hydraulic control treatment will be effective, as long as the suspension remains in a kinetically-trapped state for timescales consistent with commercial heat extraction.

Experiment 6 utilizes an injectate at initial volume fraction ϕ_{max} with further pretreatment to achieve this state. The vacuum-filtered microgel suspension is converted into the shrunken state by heating them to 65ºC. Since the microgels shrink by releasing the water previously held within the volume of the polymer network, the shrunken-state suspension can be concentrated by removing the evacuated water before the injectate is loaded into the 5-mL injection loop at 55ºC. In this concentrated state, the microgels can be transported into a cold region where they will swell (Fig. 5), but will not swell to their maximum volume, because of interference from their neighbouring microspheres.

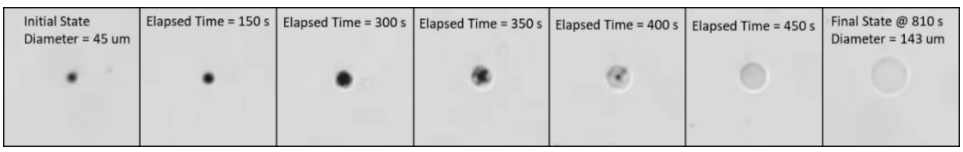

Figure 5: Volume-phase-transition of a microgel from shrunken to swollen state.

3.2. Process Flow Diagram

The bench-scale, microfluidic system employed in this study consisted of branching conduits and non-isothermal temperatures (Fig. 6). This design is intended to provide low-temperature, low-pressure "proof-of-concept" experiments that mimic an EGS reservoir that happens to experience short-circuited behavior and premature thermal breakthrough. The setup utilizes the Vapourtec Series E flow chemistry system, which consists of a "next-generation" peristaltic pump and two, temperature-controlled coiled-tube reactors with volumes of 5 mL and 10 mL and inner diameter of 0.8 mm. The smaller coiled-tube reactor acts as the injection loop and is connected to an injection valve that enables one to introduce a specified volume of injectate into a circulating system without disrupting the hydraulic state. By turning the injection valve into "injection" mode, the suspension can be directed into the temperature-controlled, 10-mL coiled-tube reactor. Outside of the primary reactor, the process connections are kept at a certain temperature in an insulated and temperature-controlled 1/16" outer diameter and 0.8 mm inner diameter PTFE (i.e., Teflon) tube. The temperatures of the process connections are controlled by PID controllers connected to heating cords that line the PTFE tubes.

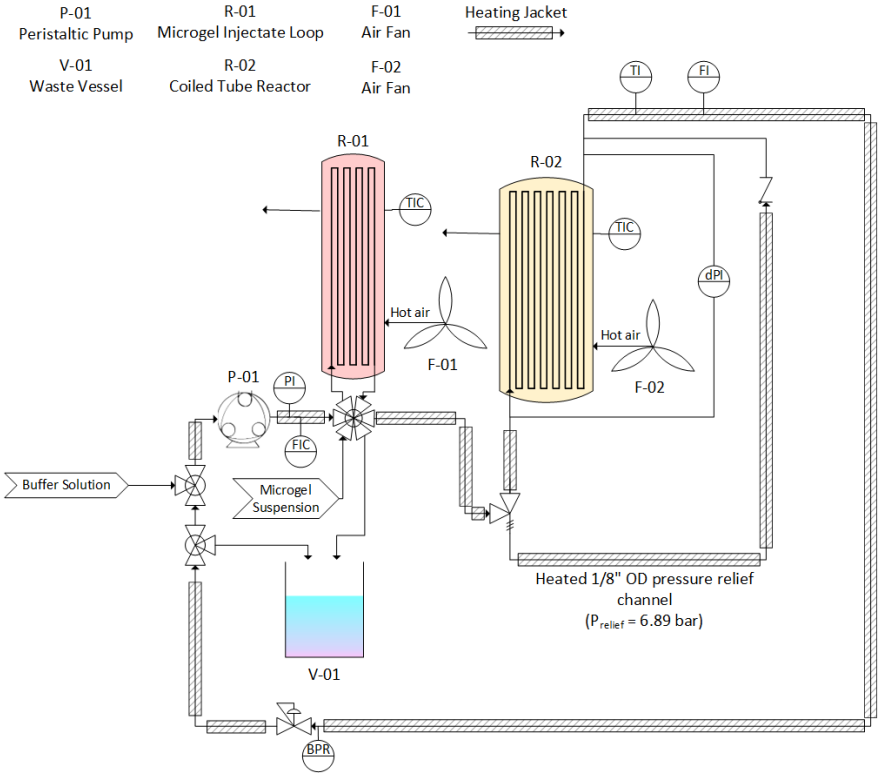

Figure 6: Process Flow Diagram of microfluidic setup used in microgel suspension pulse injection test. Vapourtec equipment includes R-01, F-01, R-02, F-02, P-01, BPR, and instrumentation associated with them.

Table 2: Microfluidic system equipment specifications corresponding to Figure 6

Equipment Code	Equipment	Specifications			
		Volume [mL]	Inner diameter [mm]	Temperature control	Miscellaneous
R-01	Microgel injection loop	5.5	0.8	Yes – Vapourtec	Stainless steel
R-02	Coiled tube reactor	10	0.8	Yes – Vapourtec	Stainless steel P_{max} =10 bar
	Tubing	3.23	0.8	Yes – PID controller	PTFE
	Bypass line	1.4	1.5	Yes – PID controller	PTFE, P_{bypass} = 6.89 bar

To mimic the behavior of multiple flow paths in a geothermal system, the experimental setup includes a "bypass" flow path that enables circulating fluids to be redirected around the 10 ml coiled-tube reactor after the hydraulic control treatment is applied. To force 100% of circulating fluids to initially flow through the primary reactor, a 6.89 bar pressure relief valve is situated before the inlet to the reactor. As a result, the bypass flow path can only be activated if the hydraulic control treatment induces a frictional power loss that results in pressure near the reactor inlet reaching greater than 6.89 bar. The bypass channel is a circular Teflon tube with 1/8" outer diameter and 1.5 mm inner diameter. Its temperature is maintained at $T > T_{LCST}$. A check valve is installed at the end of the bypass channel to prevent backflow where it reconnects with the circulation system.

Transient differential pressures were recorded across the primary reactor. An Alicat P-Series Differential pressure indicator is installed such that it measures the frictional pressure drop between the inlet and outlet of the 10 ml coiled-tube reactor and an Alicat CODA Coriolis mass flowmeter is situated downstream of the position where the bypass channel reconnects to the circulation system. A backpressure regulator (BPR) is used to maintain a system pressure greater than 2.0 bar, which is large enough to prevent the formation of gas bubbles. The total system volume excluding the injection loop is roughly 13.5 ml which results in a system residence time of 4.5 minutes at a volumetric flow rate of 3 ml/min. With the system in "inject" mode, the total system volume temporarily increases to 19 ml because of the extra 5.5 mL introduced by the injection loop.

3.3. Experiments One through Five

Frictional power loss measurements were determined while flowing an injectate at a specified concentration into the microfluidic system. This allowed for the measurement of varying injection conditions on mass flow rate and pressure drop of the circulating suspension. This experiment is prepared by circulating a simulated geothermal brine using pH 6 buffer solution throughout the microfluidic setup. The volumetric flow rate under initial conditions is set at a value of 3 mL/min which is accomplished by specifying the peristaltic pump to operate at a factory-calibrated rotational frequency. The tube heating jackets are inactive and the 10 ml coiled tube reactor is kept at temperature of 25°C. Meanwhile, the bypass line is kept at a constant temperature of 55°C. After setting these parameters, the flow rate, pressure, and temperature of the system are allowed to stabilize for 15 minutes to reach hydrostatic equilibrium. The system is then kept running for another 15 – 30 minutes to collect baseline data measurements of mass flow rate and pressure loss. Table 3 describes the operational conditions corresponding to experiments one through five. Baseline frictional power loss ($\dot{E}_0$) is determined via Eq. 1 using the average of these measurements. Relative frictional power loss ($\dot{E}_r$) is then calculated as:

$$\dot{E}_r = \frac{\dot{E}}{\dot{E}_0} \tag{5}$$

Table 3: Operational conditions of frictional power loss experiment

Parameter	Value
Baseline volumetric flow rate	3 mL/min
Baseline system pressure	2 – 2.1 bar_g
Coiled tube reactor temperature	25°C
Injection loop temperature	25°C
Main circulation heating jacket temperature	Room temperature
Bypass line temperature	55°C
Residence time	4.5 minutes
Circulating fluid	pH 6 solution of water and sodium phosphate
Injectate volume fraction (ϕ)	$0.03\phi_{max}$, $0.1\phi_{max}$, $0.3\phi_{max}$, $0.5\phi_{max}$, ϕ_{max}
Injectate vial temperature	Room temperature, 65°C for ϕ_{max}

Injectate is loaded into the injection loop with a 12 ml syringe. This loading process displaces the existing buffer solution present in the loop into the waste vessel (V-01) and replaces it with the injectate. The injection process begins by turning the injection valve into "inject" mode. During this process, the main circulation connects with the injection loop and the circulating buffer solution pushes the injectate pulse into the main circulation system. After 3 minutes, injection is terminated by switching the injection valve back to "load" mode, which hydraulically isolates the injection loop from the main circulation system. Mass flow rate and frictional pressure drop after the injection are then recorded and frictional power loss is calculated assuming a constant mass density.

3.4. Experiments Six

Table 4: Operational conditions of Experiment Six

Parameter	Value
Baseline volumetric flow rate	3 mL/min
Baseline system pressure	2 – 2.1 bar_g
Coiled tube reactor temperature	25°C
Injection loop temperature	55°C
Main circulation heating jacket temperature	55°C
Bypass line temperature	55°C
Residence time	4.5 minutes
Circulating fluid	pH 6 solution of water and sodium phosphate
Injectate vial temperature	65°C

The final experiment (i.e., Experiment Six) investigated the potential of injecting the hydrogel microsphere suspension in the shrunken-state so that a more tightly-packed concentration of particles can be introduced into the cooled region. The setup of this experiment is similar with Experiment One through Five. The main difference of this experiment is keeping the main circulation line heating jacket, bypass line, and the injection loop at temperature of 55°C to keep the microgels in the shrunken state outside of the reactor. Table 4 describes the operational conditions of the frictional power loss experiment.

The injectate is prepared as described in subsection 3.1 to allow underswollen microgels to swell and occupy higher volume fractions of the cooled reactor than the injectate at ϕ_{max} consisting of swollen microgels. 6 mL of shrunken microgels are loaded into the heated injection loop. The injection valve is closed to the "load" mode after 5.7 minutes, accounting for the possibility of slower mass flow rate following the jamming in the reactor and evacuation into the bypass line. Mass flow rate and pressure drop after the injection are recorded to evaluate their time evolution until jamming and flow redistribution is achieved.

With the microfluidic setup described in Figure 6, jamming and flow redistribution can be identified through measurements of pressure drop, mass flow rate, and system pressure. A jam in the coiled tube reactor should stop fluid flow in the reactor, reducing the pressure drop in the reactor until it reaches 0. As the peristaltic pump keeps pushing fluid into the jammed reactor, system pressure should increase until it passes the bypass line pressure relief threshold (P_{bypass}). Above this pressure, the circulating fluid should be able to flow into the bypass line and continue its circulation, keeping the system pressure above P_{bypass} but still below Vapourtec's safety trip pressure (P_{trip}). Mass flow rate should not reduce to zero, however, as fluid flowing through the bypass line should be able to be recorded by the Coriolis mass flowmeter past the bypass line. These changes of the measured parameters should not revert to baseline after the injection valve is closed.

4. RESULTS AND DISCUSSION

4.1 Experiments One through Five

This subsection describes the results of the first five experiments which consisted of injection volume fractions of $0.03\phi_{max}$, $0.1\phi_{max}$, $0.3\phi_{max}$, $0.5\phi_{max}$, and ϕ_{max}. These injectates were injected into the system for 3 minutes before the injection valve is closed. The system ran at operational conditions set to the parameters described in Table 2. To evaluate their transport behavior and possibility of jamming in the coiled tube reactor, the analyses of these experiments are done at times 0 – 1.5 residence times (t_r), during which jamming is most probable, because the particles have experience minimal hydrodynamic dispersion. Assuming minimal hydrodynamic dispersion of the microgels during this timescale, the volume fractions reported here are volume fractions of the injectate as they pass through the coiled-tube reactor.

The experimental results for the first five experiments are shown in Fig. 7. The results show a monotonic increase in the frictional power loss with increasing injectate volume fractions. At injectate volume fractions of $0.03\phi_{max}$ and $0.1\phi_{max}$, a relative power loss near unity indicates that at or below $0.1\phi_{max}$, the system experiences negligible impacts related to the presence of hydrogel suspensions. At injectate volume fractions $0.3\phi_{max}$, and $0.5\phi_{max}$, the maximum relative power losses reach values of roughly 3 and 4, respectively, while at ϕ_{max} the maximum value reaches roughly 12.

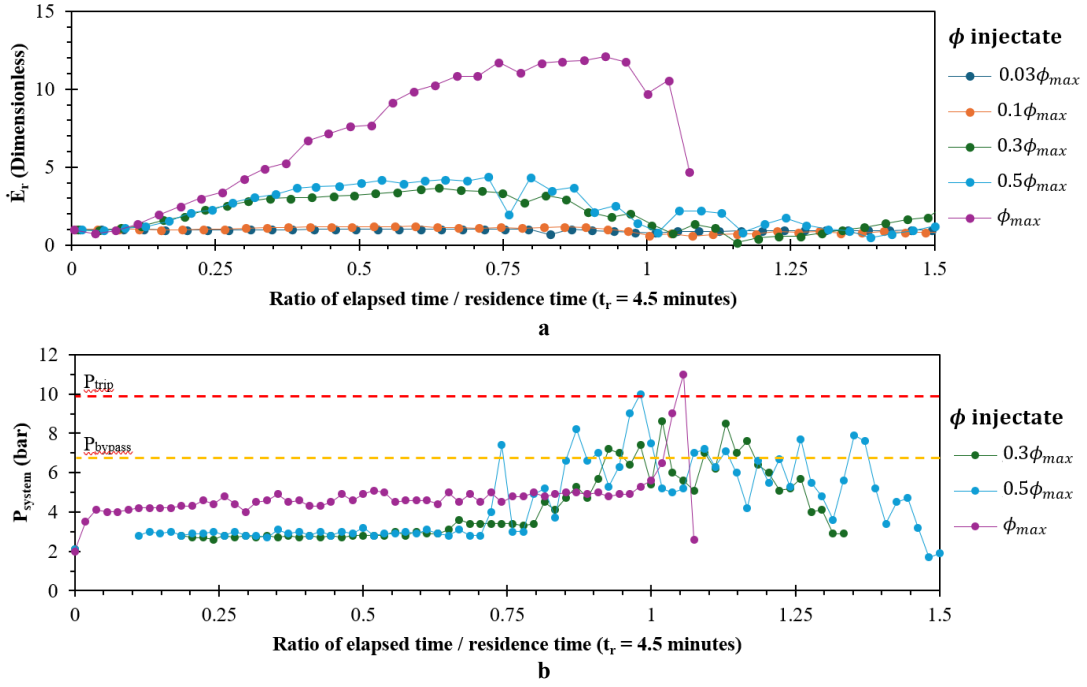

Figure 7: Evolution of $\dot{E}_r$ (a) and P_{system} (b) at different injectate ϕ at $0 \leq t \leq 1.5t_r$ and T = 25 °C. Note that a value of unity corresponds to the elapsed time before injected fluids complete a circulation and pass the injection valve

Fig. 7b shows a plot of total system pressure as a function of the number of residence times circulated. The red and yellow horizontal lines plotted at values of roughly 7 and 10 bar correspond to the minimum pressure needed to activate the bypass line and the maximum system pressure allowed before the circulation system is automatically shut off. At injectate volume fractions of $0.03\phi_{max}$ and $0.1\phi_{max}$, the system pressure never exceeded the bypass pressure. In contrast, injectate volume fractions of $0.3\phi_{max}$, $0.5\phi_{max}$, and ϕ_{max} all induced increases in system pressure to values larger than 7 bar. Although these pressure spikes exceed the bypass threshold pressure, the flow did not experience splitting between the bypass line and the primary reactor, because these momentary pressure spikes occurred when the injectate had already exited the primary reactor and passed the junction between the two flow paths.

At ϕ_{max}, the total system pressure exceeded 10 bar at a value of roughly 1.07 residence times. This observation is encouraging, because it suggests that the suspension experienced a momentary circumstance in which the microgels sufficiently block and resists flow exceeding 10 bar pressure. However, one cannot claim that this observation corresponds to a demonstration of jamming, because it occurred at a pinch-point within the mass flow meter rather than in the target system at cool temperatures. While jamming was not officially observed, these results do suggest that the hypothesis introduced earlier in this manuscript is valid; increasing the fraction of hydrogels increases the resistance to flow.

The question then emerges as to which of the scenarios presented in Fig. 3 correspond to the results of these experiments. Because the relative frictional power loss drops with increasing time, it is most likely true that the microscopic explanation for these observations is that the bulk fluid (i.e., the free water and the microspheres) remain mobile in the circulation system which supports the use of Eq. 2. The results also suggest that the flow resistance induced by the microgels up to injectate volume fraction ϕ_{max} do not produce pressure exceeding 7 bar. This is true, because the circulation system was able to push the concentrated suspension outside of the primary reactor. Therefore, introducing a bypass line with a lower pressure relief valve may be necessary to demonstrate complete jamming.

Figure 8 plots the maximum relative frictional power loss for the first five experiments as function of volume fraction. The results indicate a positively correlated relationship with volume fraction, with an R^2 value of 0.975. Assuming that the microgels flow with the suspension, a power-law relationship between microgel volume fraction ϕ and momentum diffusivity D_f can be determined in future expansion of this study using the equation developed by Krieger & Dougherty (1959) which involves volume fraction and apparent viscosity.

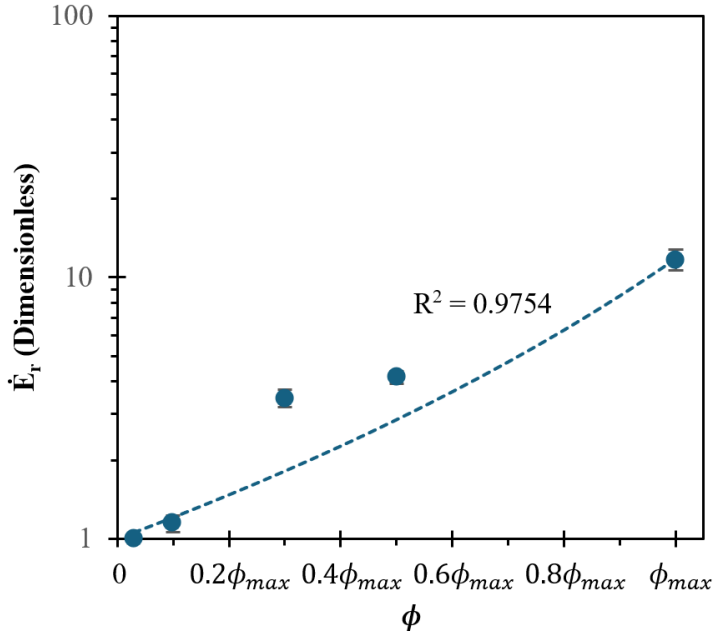

Figure 8: $\dot{E}_r$ vs. injectate ϕ during microgel deposition in the coiled tube reactor

4.2 Experiments Six

As discussed in subsection 3.4, the final experiment aimed at increasing the likelihood demonstrating jamming by injecting a concentrated suspension of hydrogel microspheres in the shrunken state. The system ran at the operational conditions specified in Table 3. The concentrated suspension was loaded into the 5-mL injection valve and then kept at elevated temperatures until the injection valve was opened. The injection valve remained open for roughly 5.7 minutes and the corresponding changes to frictional pressure drop, mass flow rate, and total system pressure were recorded (Fig. 9).

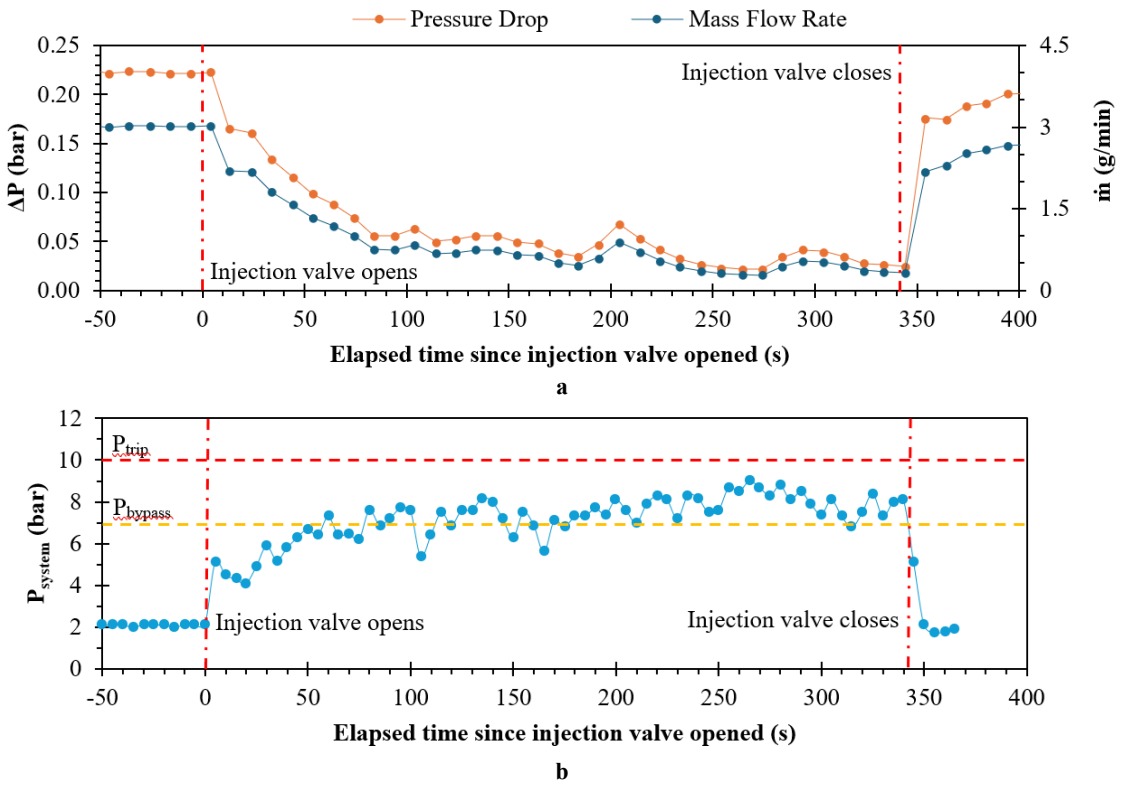

Figure 9: Evolution of $\dot{m}$, ΔP (a), and P (b) after the injection of concentrated shrunken microgel injectate

As shown in Fig. 9, this injectate preparation method led to a significant drop in the mass flow rate and the frictional pressure drop through the primary reactor. Meanwhile, total system pressure rose immediately following the start of the injection period, reached a maximum of roughly 9 bar, then fell back to the initial system pressure immediately after closing the injection valve. At first glance, the time evolutions of the pressure drop, mass flow rate, and system pressure suggest that jamming occurred in the reactor. The pressure drop in the primary reactor, for instance, reduced significantly which suggests reduced flow in the reactor. Meanwhile, total system pressure spiked to the range above the bypass line pressure threshold, indicating that circulating fluids were redirected into the bypass line. However, if circulating fluids were redirected through the bypass line, then the mass flow rate should remain constant. In addition, pressure drop, mass flow rate, and total system pressure should not return to baseline values after the injection valve was closed. Evidently, the shrunken-state suspension remained immobile in the 5 mL injection loop for the entire duration of this experiment.

These results suggest that the shrunken microgel injectate did not flow passively with the surrounding fluids. Instead, the shrunken-state suspension remained immobile in the injection valve even as liquid water continued to flow. Therefore, this injection method introduced a microscopic flow behavior consistent with the porous-media type flow depicted in Fig. 3c. Presumably, this behavior emerged as a result of reswelling of the shrunken microgels in the suspension. Therefore, improving injectate preparation with controlled, heightened temperature throughout injection process and proper agitation of the injectate could improve the results of this experiment.

5. CONCLUSION

The threat of premature thermal breakthrough significantly affects the financial uncertainty of EGS reservoirs. This work follows up on a recent proposal to induce flow redistribution out of "short-circuited" cold fractures and into still-hot flow paths. pNIPA-SA microgels have the possibility to implement this mechanism through its volume-phase-transition characteristics by "jamming" cooled fractures and forcing fluid flow to channels with better heat transfer properties.

The work presented here investigated methodologies for injecting such particles into the subsurface and evaluated the success of the subsequent impacts. In a bench-scale microfluidic setup, this work showed that the frictional power loss of the circulating suspension increases with increasing injectate concentration. However, injectate prepared at volume fraction up to the maximum possible volume fraction post-treatment, ϕ_{max} did not induce jamming, because the system pressure affected by the microgels was less than the 7 bar pressure relief valve. An effort to overcome this limitation by injecting the particles in the shrunken state failed to yield adequate results, because the shrunken-state particles were in an immobile state in the injection loop. The shrunken-state microspheres were suspended in deionized water, however, so future work should determine if such behaviors can be prevented by inhibiting microgel aggregation.

In future work, additional frictional power loss experiments will be performed to determine which microscopic behaviors emerge when the rating of the pressure relief valve is less than the yield stress of the suspension. The behavior of these hydrogel microspheres will also be explored under additional variables, such as confining pressure, temperature, flow path size/geometry, and more. Finally, similar experiments will be performed with microspheres prepared under evolving synthesis conditions.

6. ACKNOWLEDGEMENTS

This material is based up on work supported by the U.S. Department of Energy 's Office of Energy Efficiency and Renewable Energy (EERE) under the Geothermal Technologies Office, Award Number DE-EE0009786. The views expressed herein do not necessarily represent the view of the U.S. Department of Energy or the United States Government. We extend our gratitude to the Indonesia Endowment Fund for Education (LPDP) for the financial support of this research. We thank a member of our research team, Daniel Korzukhin, for his contributions to this research.

REFERENCES

Baxter, A. M., Tang, D., Hawkins, A. J., Wiesner, U. B., Fulton, P. M., Alabi, C. A., Tester, J. W., Hormozi, S. (2023). *The Rheology of Temperature-Responsive Volume-Phase Transition Hydrogels for the Improved Thermal Performance and Lifetime of Geothermal Reservoirs*.

Fox, D. B., Koch, D. L., & Tester, J. W. (2015). The effect of spatial aperture variations on the thermal performance of discretely fractured geothermal reservoirs. *Geothermal Energy*, *3*(1), 1–29. https://doi.org/10.1186/s40517-015-0039-z

Hawkins, A. J. (2024). *Hydrodynamic Dual Space Yields a Prediction of the Muon Magnetic Moment Anomaly with Better Accuracy than the Standard Model*. https://doi.org/10.26434/chemrxiv-2024-zqnx4

Hawkins, A. J., Tang, D., Baxter, A. M., Puthur, R., Korzukhin, D. T., Zody, Z. J., Abdulaziz, B. H., Fulton, P. M., Hormozi, S., Alabi, C. A., Wiesner, U. B., Tester, J. W., & Fredrick, R. (2024). *Active Tracers for Hydraulic Control of Cooled Short Circuits: Bench-Scale Demonstration and Numerical Simulation*.

Hawkins, A. J., Tang, D., Sinha, R., Fulcher, S. A., Hormozi, S., Fulton, P. M., Alabi, C. A., Wiesner, U. B., Tester, J. W., & Fredrick, R. (2023). *Active Tracers for Hydraulic Control of Cooled Short Circuits*.

Krieger, I. M., & Dougherty, T. J. (1959). A Mechanism for Non-Newtonian Flow in Suspensions of Rigid Spheres. *Transactions of the Society of Rheology*, *3*(1), 137–152. https://doi.org/10.1122/1.548848

McLean, M. L., & Espinoza, D. N. (2023). Thermal destressing: Implications for short-circuiting in enhanced geothermal systems. *Renewable Energy*, *202*, 736–755. https://doi.org/10.1016/j.renene.2022.11.102

Minami, S., Watanabe, T., Suzuki, D., & Urayama, K. (2016). Rheological properties of suspensions of thermo-responsive poly(N-isopropylacrylamide) microgels undergoing volume phase transition. *Polymer Journal*, *48*(11), 1079–1086. https://doi.org/10.1038/pj.2016.79

Shibayama, M., & Tanaka, T. (1993). *Volume Phase Transition and Related Phenomena of Polymer Gels*.

Shu, R., Sun, W., Liu, Y., Wang, T., Wang, C., Liu, X., & Tong, Z. (2013). The jamming and unjamming transition in poly(N-isopropylacrylamide) microgel suspensions. *Colloids and Surfaces A: Physicochemical and Engineering Aspects*, *436*, 912–921. https://doi.org/10.1016/j.colsurfa.2013.08.031

Tanaka, T. (1978). *PHYSICAL REVIEW LETTERS Collapse of Gels and the Critical Endpoint* (Vol. 40).

Tanaka, T., Fillmore, D., Sun, S.-T., Nishio, I., Swislow, G., & Shah, A. (1980). Phase Transitions in Ionic Gels. In *REVIEW LETTERS* (Vol. 45).

Yeghiazarian, L., Mahajan, S., Montemagno, C., Cohen, C., & Wiesner, U. (2005). Directed motion and Cargo transport through propagation of polymer-gel volume phase transitions. *Advanced Materials*, *17*(15), 1869–1873. https://doi.org/10.1002/adma.200401205